

COMPUTING PERSISTENCE DIAGRAM BUNDLES

ABIGAIL HICKOK

ABSTRACT. Persistence diagram (PD) bundles, a generalization of vineyards, were recently introduced as a way of studying the persistent homology of a set of filtrations parameterized by a topological space \mathcal{T} . In this paper, I present an algorithm for computing piecewise-linear PD bundles, a wide class that includes many of the PD bundles that one may encounter in practice. I give full implementation details for the case in which $\dim(\mathcal{T}) \leq 2$, and I outline the generalization to higher dimensions.

1. INTRODUCTION

Suppose one has a set $\{X(t)\}_{t \in \mathcal{T}}$ of point clouds parameterized by a topological space \mathcal{T} . For example, a time-varying point cloud is parameterized by $\mathcal{T} = \mathbb{R}$. At each $t \in \mathcal{T}$, one can construct a filtration (such as the Vietoris–Rips filtration) for $X(t)$ and compute its persistent homology (PH). More generally, one may have a *fibred filtration function*, a set $\{f_t : \mathcal{K}^t \rightarrow \mathbb{R}\}_{t \in \mathcal{T}}$ of filtrations parameterized by \mathcal{T} . The associated *persistence diagram (PD) bundle* is the space of persistence diagrams $PD(f_t)$ for all $t \in \mathcal{T}$. For example, a vineyard [1] is the special case in which \mathcal{T} is an interval in \mathbb{R} , and the persistent homology transform [13] is a special case in which $\mathcal{T} = S^d$. For more examples, see [6].

1.1. Contributions. I generalize the algorithm for computing vineyards [1] to an algorithm for efficiently computing PD bundles. We restrict to the case in which the PD bundle is *piecewise linear*. This means that \mathcal{T} is a simplicial complex, $\mathcal{K}^t \equiv \mathcal{K}$ for all $t \in \mathcal{T}$, and for every simplex $\sigma \in \mathcal{K}$, the function $f_\sigma(t) := f_t(\sigma)$ is linear on every simplex of \mathcal{T} . The restriction to piecewise-linear PD bundles allows us to take advantage of work in computational geometry such as the Bentley–Ottman planesweep algorithm [2] for finding intersections of lines in a plane. An analogous piecewise-linear restriction was made for computing vineyards in [1].

The idea of the algorithm is to partition the base space \mathcal{T} into polyhedrons and compute a PD “template” for each polyhedron. The partition is given by Proposition 2.4 ([6]). For any $t \in \mathcal{T}$, the persistence diagram $PD(f_t)$ can be computed in $O(N)$ time from the template for the polyhedron that contains t , where N is the number of simplices in \mathcal{K} .

The piecewise-linear restriction is reasonable for most applications. For example, suppose that we have a point cloud $X(t, \mu)$ whose coordinates depend on time t and a system-parameter value $\mu \in \mathbb{R}$. If the data set is obtained through either real-world data collection or through numerical simulation, then we likely only know the coordinates of the point cloud $X(t, \mu)$ at a discrete set $\{t_i\}$ of time steps and a discrete set $\{\mu_j\}$ of system-parameter values. For every (t_i, μ_j) , there is the filtration function $f_{(t_i, \mu_j)} : \mathcal{K} \rightarrow \mathbb{R}$ associated with the Vietoris–Rips filtration (or any other filtration) of $X(t_i, \mu_j)$. To obtain a fibred filtration function, let \mathcal{T} be a triangulation of $[\min t_i, \max t_i] \times [\min \mu_j, \max \mu_j]$ whose vertices are $\{(t_i, \mu_j)\}_{ij}$.

Date: October 13, 2022.

We can extend $\{f_{(t_i, \mu_j)}\}_{ij}$ to a fibered filtration function on all of \mathcal{T} by defining the filtration values of a simplex σ via linear interpolation of $\{f_{(t_i, \mu_j)}(\sigma)\}_{ij}$. By construction, the resulting PD bundle is piecewise linear.

I give full implementation details only for the case in which $\dim(\mathcal{T}) \leq 2$, but I discuss the mathematical generalization to higher dimensions in Section 3.2. When the base space \mathcal{T} is 2D, it is already an improvement over a vineyard. If $\dim(\mathcal{T}) = 2$, this means there are three parameters in total: the filtration parameter r as well as two parameters that locally parameterize \mathcal{T} . In higher dimensions, we are limited by the availability of computational geometry algorithms for working with a partition of a space into polyhedrons. When $\dim(\mathcal{T}) = 2$, the partition of \mathcal{T} into polygons can be represented by a doubly-connected edge list (DCEL) data structure, and we can use a standard point-location algorithm to locate the polygon that contains a given point. However, to the best of my knowledge, no one has generalized these yet to arbitrarily high dimensions.

1.2. Related Work. PD bundles were introduced in [6] as a generalization of vineyards [1]. The algorithm I present in this paper for computing PD bundles is a generalization of the algorithm presented in [1]. In many ways, the algorithm in this paper is also reminiscent of the Rivet algorithm for computing fibered barcodes of 2D multiparameter persistence modules [7].

1.3. Organization. The paper proceeds as follows. I review the relevant background on persistent homology, vineyards, and PD bundles in Section 2. I present my algorithm for computing piecewise-linear PD bundles in Section 3. Finally, I conclude and discuss possible directions for future research in Section 4.

2. BACKGROUND

We begin by reviewing persistent homology, vineyards, and PD bundles; for more details on persistent homology, see [3, 9], for more on vineyards, see [1], and for an introduction to PD bundles, see [6].

2.1. Persistent homology. Let \mathcal{K} be a simplicial complex. A *filtration function* $f : \mathcal{K} \rightarrow \mathbb{R}$ is a real-valued function on \mathcal{K} that is *monotonic*, i.e., $f(\tau) \leq f(\sigma)$ if τ is a face of σ . Monotonicity guarantees that the r -sublevel sets $\mathcal{K}_r := \{\sigma \in \mathcal{K} \mid f(\sigma) \leq r\}$ are simplicial complexes.

In persistent homology, we study how the homology of \mathcal{K}_r changes as r increases. Let $\{r_i\}$ be the image of f , ordered such that $r_i < r_{i+1}$. These are the critical values at which \mathcal{K}_r changes; for $r \in [r_i, r_{i+1})$, we have $\mathcal{K}_r = \mathcal{K}_{r_i}$. For every $i \leq j$, the inclusion $\iota_*^{i,j} : \mathcal{K}_{r_i} \hookrightarrow \mathcal{K}_{r_j}$ induces a map $\iota_*^{i,j} : H_*(\mathcal{K}_{r_i}, \mathbb{F}) \rightarrow H_*(\mathcal{K}_{r_j}, \mathbb{F})$ on homology. For the remainder of this paper, we compute homology over the field $\mathbb{F} = \mathbb{Z}/2\mathbb{Z}$. The *p*th-persistent homology (PH) is the pair

$$\left(\{H_p(\mathcal{K}_{r_i}, \mathbb{F})\}_{1 \leq i \leq N}, \{\iota_*^{i,j}\}_{1 \leq i < j \leq N} \right).$$

A homology class is *born* at r_i if it is not in the image of $\iota_*^{i,i-1}$. The homology class *dies* at $r_j > r_i$ if j is the minimum index such that $\iota_*^{i,j}$ maps it to zero. (Such a j may not exist; in that case, the homology class never dies.) The Fundamental Theorem of Persistent Homology yields compatible choices of bases for the vector spaces $H_p(\mathcal{K}_{r_i}, \mathbb{F})$. The generators in our definition of a persistence diagram, below, are the basis elements in the decomposition given by the Fundamental Theorem of Persistent Homology.

Persistent homology is often visualized as a *persistence diagram* (PD). The p th persistence diagram $PD_p(f)$ is a multiset of points in the extended plane $\overline{\mathbb{R}}^2$ that summarizes the p th persistent homology. It contains the diagonal (for technical reasons) and one point for every generator. If a generator is born at b and dies at d , then the coordinates of the corresponding point in the PD are (b, d) , and if the generator is born at b and never dies, then the coordinates of the point are (b, ∞) .

One of the standard methods for computing PH is the algorithm introduced in [4]. The algorithm requires a choice of compatible *simplex ordering* $\alpha : \mathcal{K} \rightarrow \{1, \dots, N\}$, where N is the number of simplices in \mathcal{K} . We require that $\alpha(\sigma) < \alpha(\tau)$ if $f(\sigma) < f(\tau)$ or σ is a face of τ . A compatible ordering α exists because monotonicity ensures that $f(\sigma) \leq f(\tau)$ if σ is a face of τ .

Let D be the boundary matrix compatible with this ordering. That is, let D be the matrix whose (i, j) th entry is

$$D_{ij} = \begin{cases} 1, & \alpha^{-1}(i) \text{ is a face of } \alpha^{-1}(j) \\ 0, & \text{otherwise.} \end{cases}$$

We decompose the boundary matrix D into a matrix product $D = RU$ such that U is upper triangular and R is a binary matrix that is *reduced*. A binary matrix R is reduced if $low_R(j) \neq low_R(j')$ whenever $j \neq j'$ are the indices of nonzero columns in R . The quantity $low_R(j)$ is the row index of the last 1 in column j if column j is nonzero and undefined if column j is zero. An RU decomposition can be computed in $O(N^3)$ time [3, 4].

The function $low_R(j)$ is called the *pairing function*. The authors of [1] showed that the pairing function $low_R(j)$ depends only on the boundary matrix D , and not on the particular reduced binary matrix R in the decomposition $D = RU$. A pair of simplices $(\alpha^{-1}(i), \alpha^{-1}(j))$, for which $i = low_R(j)$, represents a persistent homology class. The *birth simplex* $\alpha^{-1}(i)$ creates the homology class and the *death simplex* $\alpha^{-1}(j)$ destroys the homology class. The two simplices in a pair have consecutive dimensions (i.e., if $\dim(\alpha^{-1}(i)) = p$ then $\dim(\alpha^{-1}(j)) = p + 1$). If $\dim(\alpha^{-1}(i)) = p$ and $\dim(\alpha^{-1}(j)) = p + 1$, then a point with coordinates $(f(\alpha^{-1}(i)), f(\alpha^{-1}(j)))$ is added to the p th persistence diagram. We refer to $f(\alpha^{-1}(i))$ as its *birth* and $f(\alpha^{-1}(j))$ as its *death*. Some simplices are not paired. If $i \neq low_R(j)$ for all j , then the simplex $\alpha^{-1}(i)$ is a birth simplex for a homology class that never dies. Its birth is $f(\alpha^{-1}(i))$ and its death is ∞ . If $\dim(\alpha^{-1}(i)) = p$, then a point with coordinates $(f(\alpha^{-1}(i)), \infty)$ is added to the p th persistence diagram.

2.2. Vineyards. Let \mathcal{K} be a simplicial complex. A *1-parameter filtration function* on \mathcal{K} is a function $f : \mathcal{K} \times I \rightarrow \mathbb{R}$, where $I = [t_0, t_1]$ is an interval in \mathbb{R} , such that $f(\cdot, t)$ is a filtration function on \mathcal{K} for all $t \in I$. For each $t \in I$, the r -sublevel sets $\mathcal{K}_r^t = \{\sigma \in \mathcal{K} \mid f(\sigma, t) \leq r\}$ are a filtration of \mathcal{K} . The set $\{\{\mathcal{K}_r^t\}_{r \in \mathbb{R}}\}_{t \in I}$ is a set of filtrations parameterized by $t \in I$. For each $t \in I$, one can compute the persistence diagram $PD(f(\cdot, t))$. The associated *vineyard* is the 1-parameter set $\{PD(f(\cdot, t))\}_{t \in I}$ of persistence diagrams. We visualize the vineyard in $\mathbb{R}^2 \times I$ as a continuous stack of PDs (see Figure 1). The points in the PDs trace out curves with time; these curves are the *vines*.

An algorithm for computing vineyards is given by [1], and we review it here. As in Section 2.1, we define a simplex ordering function $\alpha : \mathcal{K} \times I \rightarrow \{1, \dots, N\}$ such that $\alpha(\sigma, t) < \alpha(\tau, t)$ if $f(\sigma, t) < f(\tau, t)$ or σ is a face of τ .

Let $D(t)$ be the boundary matrix compatible with the ordering at time t . There is a corresponding pairing function $low_R(j, t)$. The simplex ordering is constant on intervals

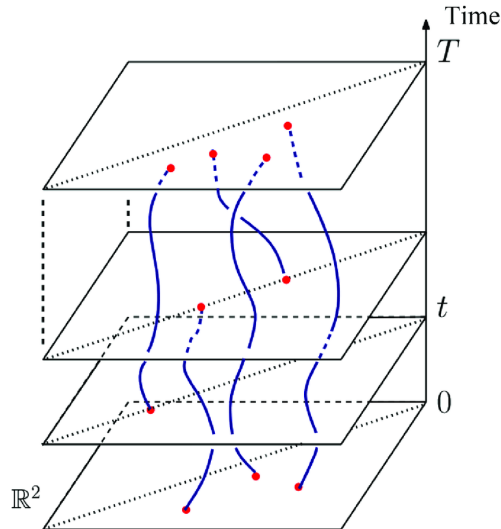


FIGURE 1. An illustration of a vineyard. There is a persistence diagram for each time t . (This figure is a slightly modified version of a figure that appeared originally in [8], which is available under a Creative Commons license.)

$J \subseteq I$ for which we have that if $f(\sigma, t) \leq f(\tau, t)$ for some $t \in J$, then $f(\sigma, s) \leq f(\tau, s)$ for all $s \in J$. On an interval J on which the simplex ordering is constant, we let $\alpha(\cdot, J) : \mathcal{K} \rightarrow \{1, \dots, N\}$ denote the simplex ordering in J . If the simplex ordering is constant in J , then so is $D(t)$, and thus so is the pairing function $low_R(j, t)$. We denote the pairing function in J by $low_R(\cdot, J)$. In order to compute the pairing function for all $t \in I$, we only need to compute the pairing function once per interval J on which the simplex ordering is constant. For all $t \in J$ and pairs i, j such that $i = low_R(j, J)$, the p th persistence diagram at time t has a point with coordinates $(f(\alpha^{-1}(i, J)), f(\alpha^{-1}(j, J)))$. For all i such that $i \neq low_R(j, J)$ for all j , the p th persistence diagram at time t has a point with coordinates $(f(\alpha^{-1}(i, J)), \infty)$.

The algorithm for computing a vineyard can be broken down into three steps:

- (1) **Compute the transposition times:** Compute the times t at which there is a change in the relative order of a pair (σ, τ) of simplices. This means there are intervals J_1, J_2 with $J_1 \cap J_2 = \{t\}$ such that the simplex ordering is constant on each J_i and $(\alpha(\sigma, J_1) - \alpha(\tau, J_1))(\alpha(\sigma, J_2) - \alpha(\tau, J_2)) < 0$.
- (2) **Compute the pairing function:** For the boundary matrix $D(t_0)$ at initial time $t = t_0$, compute an RU decomposition $D(t_0) = R(t_0)U(t_0)$, where $R(t_0)$ is a reduced binary matrix and $U(t_0)$ is upper triangular. Using the initial pairing function $low_R(\cdot, t_0)$, we compute the birth and death simplices for the persistent homology of the initial filtration $f(\cdot, t_0)$. If the i th and $(i+1)$ st simplices $\alpha^{-1}(i, t)$ and $\alpha^{-1}(i+1, t)$ are transposed at time t , we update the RU decomposition by following the case work in [1]. (Note that if there is more than one pair (σ, τ) of simplices whose relative order changes at t , then the permutation can be decomposed into a sequence of such transpositions.) At worst, updating $R(t)$ requires adding one column to another and adding one row to another—similarly for $U(t)$. The addition of columns and rows is an $O(N)$ operation, but in experiments, the authors of [1] found that updating $R(t)$ and $U(t)$ can be done in approximately constant time if one uses the sparse matrix representations that are given in [1]. After an update of the RU decomposition, we

update the birth and death simplices. At most two (birth, death) simplex pairs are updated, and these updates occur in constant time. This updating procedure yields the birth and death simplices for the filtration function $f(\cdot, t)$.

- (3) **Evaluate the PD at each time:** At time t , let J be the interval such that $t \in J$ and the simplex ordering is constant in J . For every (birth, death) simplex pair (σ_b, σ_d) for the interval J , the diagram $PD_p(f(\cdot, t))$ contains the point $(f(\sigma_b, t), f(\sigma_d, t))$ if $\dim(\sigma_b) = p$. For every p -dimensional simplex σ_b that is unpaired in J , the diagram $PD_p(f(\cdot, t))$ contains the point $(f(\sigma_b, t), \infty)$.

A special type of vineyard is a *piecewise-linear vineyard*. If we are only given $f(\sigma, t_i)$ at discrete time steps t_i , then for all i we extend $f(\sigma, t)$ to $t \in [t_i, t_{i+1}]$ by linear interpolation. In this case, one can perform step (1) of the algorithm above by using the Bentley–Ottman planesweep algorithm [2]. This is because computing when (if) two simplices σ, τ get transposed in $[t_i, t_{i+1}]$ is equivalent to finding the intersection (if it exists) between the lines

$$y = \frac{f(\sigma, t_{i+1}) - f(\sigma, t_i)}{t_{i+1} - t_i}(t - t_i) + f(\sigma, t_i),$$

$$y = \frac{f(\tau, t_{i+1}) - f(\tau, t_i)}{t_{i+1} - t_i}(t - t_i) + f(\tau, t_i).$$

2.3. PD bundles. PD bundles were introduced in [6] as a generalization of vineyards in which a set of filtrations is parameterized by a base space \mathcal{T} . A vineyard is the special case in which \mathcal{T} is an interval in \mathbb{R} .

Definition 2.1. A fibered filtration function is a set $\{f_t : \mathcal{K}^t \rightarrow \mathbb{R}\}_{t \in \mathcal{T}}$ of filtration functions parameterized by a topological space \mathcal{T} . When $\mathcal{K}^t \equiv \mathcal{K}$ for all $t \in \mathcal{T}$, we define $f(\sigma, t) := f_t(\sigma)$ for all $\sigma \in \mathcal{K}$ and $t \in \mathcal{T}$.

Definition 2.2. Let $\{f_t : \mathcal{K}^t \rightarrow \mathbb{R}\}_{t \in \mathcal{T}}$ be a fibered filtration function. The topological space \mathcal{T} is the base space. The space $E := \{(t, z) \mid z \in PD_p(f_t), t \in \mathcal{T}\}$ is the p th total space. We give E the subspace topology inherited from the inclusion $E \hookrightarrow \mathcal{T} \times \overline{\mathbb{R}^2}$. The associated p th PD bundle is the triple (E, \mathcal{T}, π) , where π is the projection from E to \mathcal{T} .

In [1], it was computationally easier to work with a piecewise-linear vineyard, which is a vineyard for a fibered filtration function $f : \mathcal{K} \times [t_0, t_1] \rightarrow \mathbb{R}$ in which $f(\sigma, \cdot)$ is piecewise linear for all $\sigma \in \mathcal{K}$. (See the discussion at the end of Section 2.2.) Below, we define an analog of piecewise-linear vineyards.

Definition 2.3 (Piecewise-linear PD bundles). Let $\{f_t : \mathcal{K}^t \rightarrow \mathbb{R}\}_{t \in \mathcal{T}}$ be a fibered filtration function in which $\mathcal{K}^t \equiv \mathcal{K}$. As before, we define $f(\sigma, t) := f_t(\sigma)$ for all $\sigma \in \mathcal{K}$ and $t \in \mathcal{T}$. If \mathcal{T} is a simplicial complex and $f(\sigma, \cdot)$ is linear on each simplex of \mathcal{T} for all simplices $\sigma \in \mathcal{K}$, then f is a piecewise-linear fibered filtration function. The resulting PD bundle is a piecewise-linear PD bundle.

For example, in the introduction we considered a point cloud $X(t, \mu)$ whose coordinates depended on time $t \in \mathbb{R}$ and system-parameter value $\mu \in \mathbb{R}$. Given only the coordinates of the point cloud at a discrete set $\{t_i\}$ and a discrete set $\{\mu_j\}$, we had a filtration function $f_{(t_i, \mu_j)}$ for every (t_i, μ_j) . We extended this to a piecewise-linear fibered filtration function on $\mathcal{T} = [\min t_i, \max t_i] \times [\min \mu_j, \max \mu_j]$ via linear interpolation of the filtration values for each simplex $\sigma \in \mathcal{K}$.

More generally, suppose we are given a fibered filtration function $f : \mathcal{K} \times \prod_{i=1}^m \mathcal{I}_i \rightarrow \mathbb{R}$, where each \mathcal{I}_i is a finite subset of \mathbb{R} , and we wish to extend f to a fibered filtration function whose base is $\mathcal{T} = \prod_{i=1}^m [\min \mathcal{I}_i, \max \mathcal{I}_i]$ (e.g., in the example given above, we had $\mathcal{I}_1 = \{t_i\}$ and $\mathcal{I}_2 = \{\mu_j\}$). First, we construct a triangulation \mathcal{T} (i.e., an m -dimensional simplicial complex) of $\prod_{i=1}^m [\min \mathcal{I}_i, \max \mathcal{I}_i]$ whose set of vertices is $\prod_{i=1}^m \mathcal{I}_i$. (See Appendix A.2.) Then, one can extend f to a piecewise-linear fibered filtration function $f : \mathcal{K} \times \mathcal{T} \rightarrow \mathbb{R}$ by linearly interpolating $f(\sigma, \cdot)$ on each simplex $T \in \mathcal{T}$ for all simplices $\sigma \in \mathcal{K}$.

In [6], I showed that if $f : \mathcal{K} \times \mathcal{T} \rightarrow \mathbb{R}$ is a piecewise-linear fibered filtration function on an n -dimensional simplicial complex \mathcal{T} , then \mathcal{T} can be partitioned into n -dimensional polyhedrons such that within each polyhedron P , there is a “template” from which $PD_p(f(\cdot, t))$ can be computed for all $t \in P$. The template is a list of (birth, death) simplex pairs (σ_b, σ_d) .

To make this more precise, we define

$$I(\sigma, \tau) := \{t \in \mathcal{T} \mid f(\sigma, t) = f(\tau, t)\}.$$

For every n -simplex T in \mathcal{T} , the intersection $I(\sigma, \tau) \cap T$ is \emptyset , T , a vertex of T , or the intersection of an $(n-1)$ -dimensional hyperplane with T . The set

$$(1) \quad \bigcup_{T \in \mathcal{T}} \partial T \cup \{I(\sigma, \tau) \cap T \mid I(\sigma, \tau) \cap T \text{ is } (n-1)\text{-dimensional}\}$$

partitions \mathcal{T} into polyhedrons, where T denotes an n -simplex of \mathcal{T} and ∂T denotes the boundary of T .

As in Section 2.1, we define a simplex ordering function $\alpha : \mathcal{K} \times \mathcal{T} \rightarrow \mathbb{R}$ such that $\alpha(\sigma, t) < \alpha(\tau, t)$ if $f(\sigma, t) < f(\tau, t)$ or $\sigma \subseteq \tau$. If there is a $t \in \mathcal{T}$ such that $f(\sigma, t) = f(\tau, t)$ and neither $\sigma \subseteq \tau$ nor $\tau \subseteq \sigma$, then the ordering $\alpha(\cdot, t)$ is not uniquely defined. For consistency over the base space, we fix some “intrinsic ordering” $\beta : \mathcal{K} \rightarrow \{1, \dots, N\}$ such that $\beta(\sigma) < \beta(\tau)$ if $\sigma \subseteq \tau$. We now fix $\alpha : \mathcal{K} \times \mathcal{T} \rightarrow \{1, \dots, N\}$ to be the unique simplex ordering function such that $\alpha(\sigma, t) < \alpha(\tau, t)$ if $f(\sigma, t) < f(\tau, t)$ or $\beta(\sigma) < \beta(\tau)$.

Proposition 2.4 ([6]). *If $f : \mathcal{K} \times \mathcal{T} \rightarrow \mathbb{R}$ is a piecewise-linear fibered filtration function, then the set in Equation 1 partitions \mathcal{T} into polyhedra P on which the simplex ordering is constant (i.e., $\alpha(\sigma, \cdot)|_P$ is constant for all $\sigma \in \mathcal{K}$). Therefore the set of (birth, death) simplex pairs for f is constant within each P .*

3. COMPUTING PIECEWISE-LINEAR PD BUNDLES

The algorithm for computing a piecewise-linear PD bundle is split into three main steps:

- (1) **Compute the polyhedrons:** Compute the polyhedrons on which the simplex ordering (and thus pairing function) is constant (see Prop 2.4). For every pair of adjacent polyhedrons, there is a permutation π that relates the differing simplex orders in each polyhedron. We compute and record the list of simplex pairs (σ, τ) such that π changes the relative positions of σ and τ . In the “generic case,” (defined below at the beginning of Section 3.1.1), π is the transposition of a single pair (σ, τ) of simplices with consecutive indices in the simplex ordering.
- (2) **Compute the pairing function:** Choose a point $t_* \in \mathcal{T}$. Compute the simplex ordering at t_* , the boundary matrix $D(t_*)$, and an RU decomposition $D(t_*) = R(t_*)U(t_*)$, where $R(t_*)$ is a reduced binary matrix and $U(t_*)$ is upper triangular. We traverse the polyhedrons, starting with the polyhedron that contains t_* . As we move from one polyhedron to the next, we perform the simplex permutation π computed

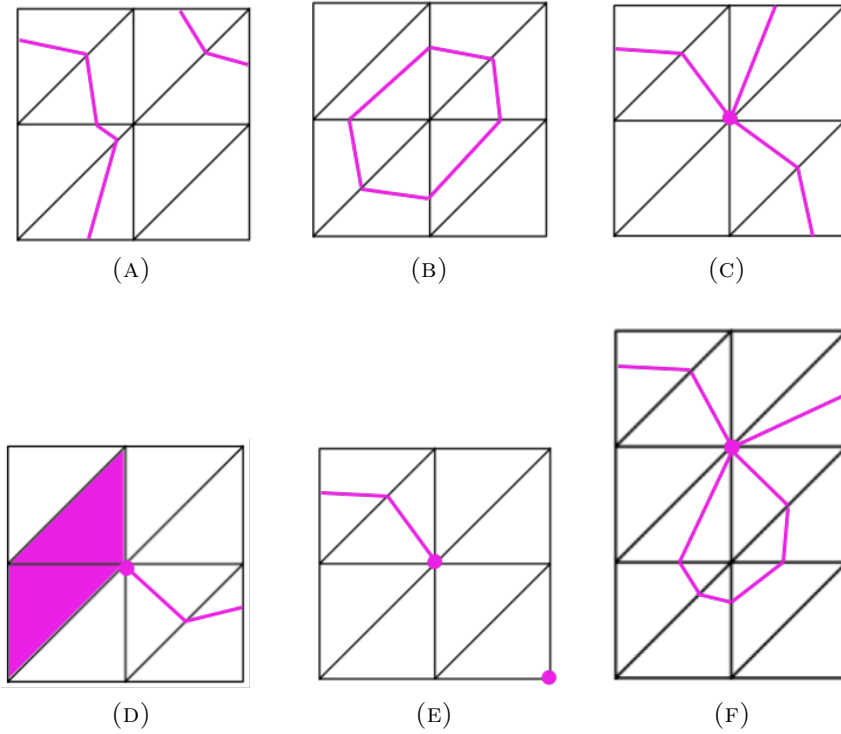


FIGURE 2. A few possible cases for the set $I(\sigma, \tau)$, in pink. The black lines are the 1-skeleton of \mathcal{T} .

above. We update the RU decomposition and pairing function via the update rules that are used when computing vineyards (see [1]). In each polyhedron, we store its pairing function (i.e., the pairs (σ_b, σ_d) of birth and death simplex pairs and also the unpaired simplices σ_b , which are birth simplices for homology classes that never die).

- (3) **Query the PD bundle:** To see the p th persistence diagram $PD_p(f(\cdot, t))$ associated with point $t \in \mathcal{T}$, first locate the polyhedron P that contains t . For each pair (σ_b, σ_d) of simplices in the pairing function for P , the diagram $PD_p(f(\cdot, t))$ has a point with coordinates $(f(\sigma_b, t), f(\sigma_d, t))$ if $\dim(\sigma_b) = p$. For every p -dimensional simplex σ_b that is unpaired in P , the diagram $PD_p(f(\cdot, t))$ contains the point $(f(\sigma_b, t), \infty)$.

Steps 1–3 are directly analogous to steps 1–3 in the algorithm for computing vineyards that was presented in Section 2.2. In what follows, I elaborate on each step of the algorithm above. We focus on the case in which \mathcal{T} is 2D.

3.1. Special case: \mathcal{T} is 2-dimensional. Let \mathcal{K} be a simplicial complex, let $f : \mathcal{K} \times \mathcal{T} \rightarrow \mathbb{R}$ be a piecewise-linear fibered filtration function, and suppose \mathcal{T} is 2D. If T is a triangle in \mathcal{T} , then $I(\sigma, \tau) \cap T$ is one of \emptyset , T , a vertex of T , or a line segment whose endpoints are on ∂T . In Figure 2, we show a few possible cases for $I(\sigma, \tau)$. The set in Equation 1 is a set L of line segments, and the planar subdivision induced by L is a *line arrangement* $\mathcal{A}(L)$. For example, see Figure 3.

For ease of exposition, we will make two genericity assumptions for the remainder of Section 3.1. The idea of the algorithm is not different in the general case, but it requires

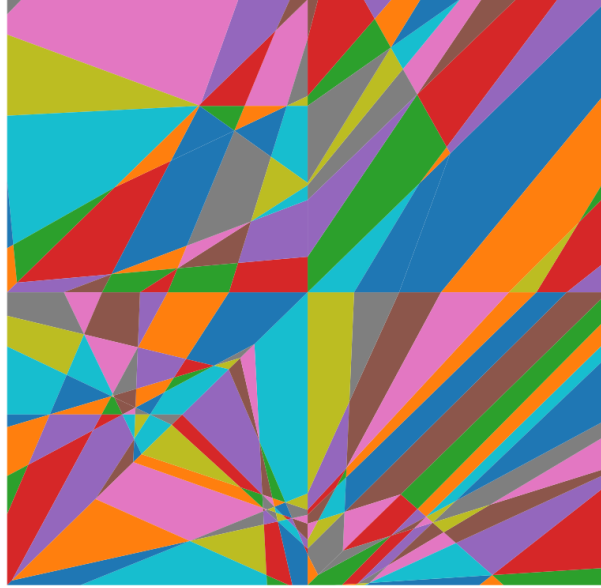


FIGURE 3. A line arrangement $\mathcal{A}(L)$ that represents the partition of a triangulated base space \mathcal{T} into polygons (see Proposition 2.4). Within each polygon, the simplex ordering is constant. (This figure appeared originally in [6].)

some technical modifications, which I discuss in Appendix A.1. The assumptions are as follows:

- (1) For all distinct simplices $\sigma, \tau \in \mathcal{K}$ and all vertices $v \in \mathcal{T}$, we have that $f(\sigma, v) \neq f(\tau, v)$. This implies that for all triangles $T \in \mathcal{T}$, the intersection $I(\sigma, \tau) \cap T$ is either \emptyset or a line segment whose endpoints are not vertices of T . For examples, see Figures 2a and 2b.
- (2) For all distinct simplices $\sigma_1, \tau_1, \sigma_2, \tau_2 \in \mathcal{K}$ and every triangle $T \in \mathcal{T}$ such that $I(\sigma_1, \tau_1) \cap T$ and $I(\sigma_2, \tau_2) \cap T$ are nonempty, the line segments $I(\sigma_1, \tau_1) \cap T$ and $I(\sigma_2, \tau_2) \cap T$ do not share any endpoints.

3.1.1. *Computing the polygons.* For a piecewise-linear vineyard, computing the intervals on which the simplex ordering is constant can be reduced to finding the intersections between the piecewise-linear functions $y = f(\sigma, t)$ and $y = f(\tau, t)$ for all pairs (σ, τ) of simplices in \mathcal{K} . Likewise for a piecewise-linear PD bundle, computing the polygons on which the simplex ordering is constant can be reduced to finding the intersections $I(\sigma, \tau)$ for all pairs (σ, τ) of simplices.

Definition 3.1. *Let ℓ be a line segment whose endpoints are on the boundary of a triangle T in \mathcal{T} . The line segment ℓ partitions \mathcal{T} into polygons Q_1 and Q_2 . We say that simplices $\sigma, \tau \in \mathcal{K}$ swap along ℓ if $(\alpha(\sigma, t_1) - \alpha(\tau, t_1))(\alpha(\sigma, t_2) - \alpha(\tau, t_2)) < 0$ for all $t_1 \in Q_1$ and $t_2 \in Q_2$ (i.e., σ and τ have different relative orders in Q_1 and Q_2).*

Under the generic assumptions we made earlier, a pair (σ, τ) swaps along ℓ if and only if $\ell = I(\sigma, \tau) \cap T$ for a triangle $T \in \mathcal{T}$. (See Lemma A.3 for a discussion of the general case.)

We wish to compute the line arrangement $\mathcal{A}(L)$, where L is the set of line segments defined by Equation 1. (See Figure 3.) The polygons of $\mathcal{A}(L)$ are the polygons on which

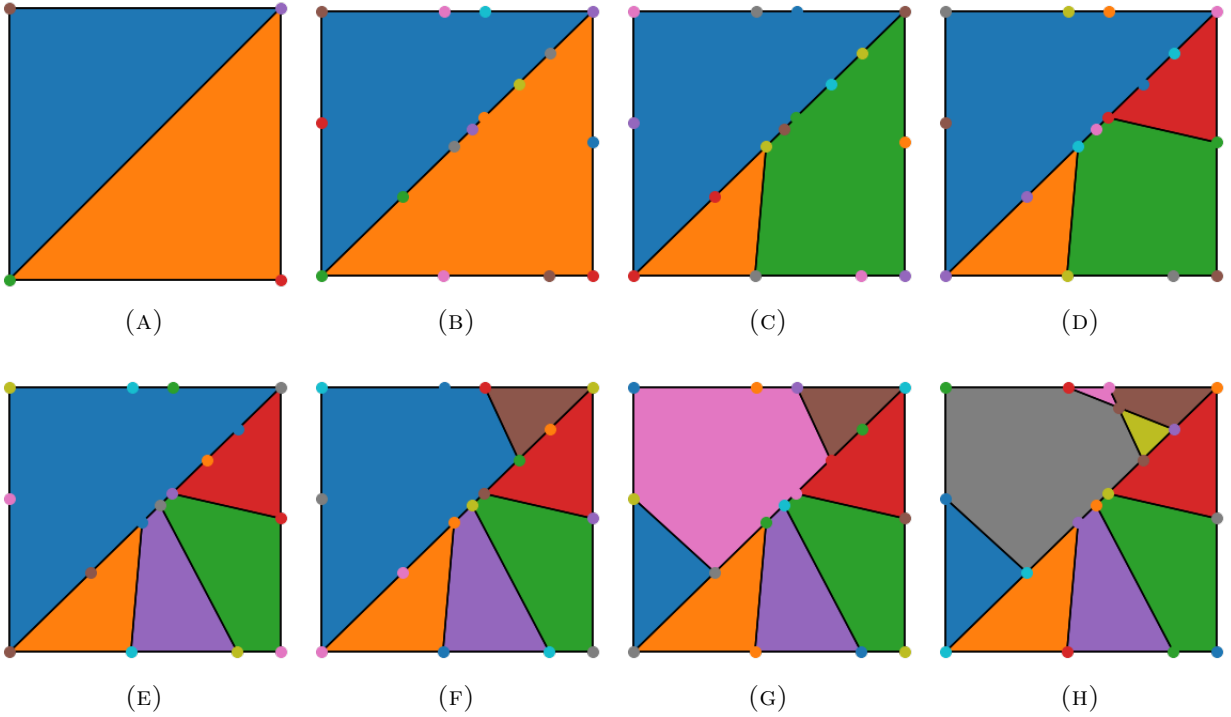


FIGURE 4. Computing the polygons. (A) The line arrangement $\mathcal{A}(L)$ is initialized to represent the triangulated base space \mathcal{T} , which in this case consists of two triangles. (B) We find the vertices v of $\mathcal{A}(L)$ that lie on the 1-skeleton of \mathcal{T} . (C)–(H) We incrementally add the line segments of the form $I(\sigma, \tau) \cap T$ for a triangle T in \mathcal{T} . The endpoints of a given line segment are a pair (v, w) of vertices in (B).

the simplex ordering is constant. We store $\mathcal{A}(L)$ using a doubly-connected edge list (DCEL) data structure [2]. A DCEL is a standard data structure for storing a polygonal subdivision of the plane.

We compute $\mathcal{A}(L)$ using the following algorithm, illustrated in Figure 4:

- (1) We initialize $\mathcal{A}(L)$ so that it represents the triangulation \mathcal{T} . (See Figure 4a.) In addition to the usual data that a DCEL stores, we enumerate the triangles in \mathcal{T} and every half edge e stores the index of the triangle in \mathcal{T} that e is on the boundary of.
- (2) Let γ be a path through the 1-skeleton of \mathcal{T} that traverses each edge at least once. For example, suppose \mathcal{T} is a triangulation of a grid, as in Figure 5a. A path γ through \mathcal{T} is shown in Figure 5b.
- (3) The restriction of f to the path γ is a 1-parameter filtration function (the input to a vineyard). We use the Bentley–Ottman algorithm [2] to find the points v on γ at which pairs of simplices swap (i.e., the relative order of a pair of simplices changes). See Figure 4b. The points v are the points on the 1-skeleton of \mathcal{T} at which $f(\sigma, v) = f(\tau, v)$ for some $\sigma \neq \tau$. When we find a vertex v , we add it to the DCEL that represents $\mathcal{A}(L)$; we do this by splitting the edge in the DCEL that the vertex lies on. For each triangle $T \in \mathcal{T}$, we maintain a dictionary whose keys are pairs (σ, τ) of simplices. The value associated with (σ, τ) is the list of vertices v on ∂T

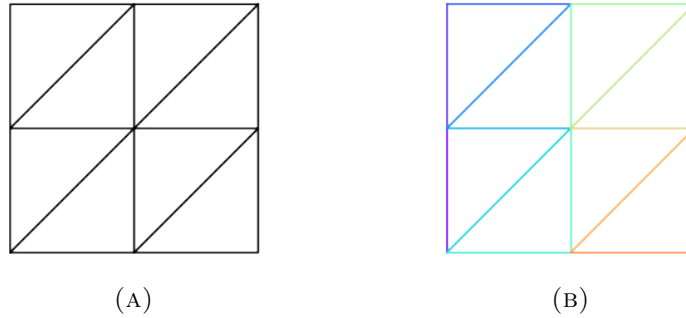


FIGURE 5. (A) A triangulated base space \mathcal{T} . (B) A path γ that traverses each edge of the 1-skeleton of \mathcal{T} , starting at the bottom-left vertical edge (violet) and ending at the top-right vertical edge (red).

at which σ and τ swap. This list is updated as we find vertices; at the end of the Bentley–Ottman algorithm, every (σ, τ) in the dictionary for T is associated with a pair (v, w) of vertices that lie on ∂T .

- (4) For each triangle $T \in \mathcal{T}$ and for each pair (σ, τ) of simplices in its dictionary, there is an associated pair (v, w) of vertices that lie on the boundary ∂T . The vertices v, w must be the endpoints of a line segment $\ell \in L$ along which (σ, τ) swap, so for each (v, w) , we add a line segment with endpoints (v, w) to the DCEL that represents $\mathcal{A}(L)$. (See Figures 4C–H.) There are many standard algorithms for doing this: one example is the incremental algorithm (see e.g., Chapter 8.3 of [2]), in which the line segments are incrementally added one at a time. The worst-case running time of the incremental algorithm is $O(n_T^2)$, where n_T is the number of line segments in triangle T . The algorithm also requires $O(n_T^2)$ space. The incremental algorithm can be parallelized over the triangles $T \in \mathcal{T}$.

In Figure 4, we illustrate the algorithm for computing the polygons.

Adding a single line segment to $\mathcal{A}(L)$ typically creates more than one new edge in $\mathcal{A}(L)$. For example, in Figure 4H, adding the last line segment creates two new edges and splits an existing edge into two edges. As we add line segments to $\mathcal{A}(L)$, we keep track of the pairs (σ, τ) of simplices that correspond to each edge. More precisely, if edge e is a subset of a line segment for the pair (σ, τ) of simplices, then e stores a reference to the pair (σ, τ) . We add the reference to (σ, τ) at the time that edge e is created in $\mathcal{A}(L)$. The two polygons adjacent to e have simplex orderings that are related via the transposition of σ and τ .

3.1.2. Computing the pairing function. Let G be the dual graph to the line arrangement $\mathcal{A}(L)$. The graph G contains a vertex v_P for every polygon P of $\mathcal{A}(L)$ and an edge between two vertices if the corresponding polygons are adjacent.

Next, we compute a path Γ that visits every vertex of G at least once. For example, see Figure 6. One way to obtain such a path is the following algorithm, used by Rivet [7]: We first compute a minimal spanning tree S for G via an algorithm such as Prim’s algorithm or Kruskal’s algorithm [11]. By performing a depth-first search of S , we obtain a path Γ that visits every edge of S at most twice. Γ may not be minimal, but has the following guarantee: If Γ^* is a path of minimal length that visits every vertex of G at least once, then $\text{length}(\Gamma) \leq 2 \times (\text{number of edges in } S) \leq 2 \times \text{length}(\Gamma^*)$.

$O(\sum_{T \in \mathcal{T}} k_T)$ space, and $O(\max_{T \in \mathcal{T}} \log k_T)$ time per query, where k_T is the number of vertices in $\mathcal{A}(L) \cap T$.

The pairing function in polygon P was precomputed in the previous step (see Section 3.1.2). For every (birth, death) pair (σ_b, σ_d) of simplices, $PD_p(f(\cdot, t))$ has a point with coordinates $(f(\sigma_b, t), f(\sigma_d, t))$ if $\dim(\sigma_b) = p$. For every unpaired p -dimensional simplex σ_b , the diagram $PD_p(f(\cdot, t))$ has a point with coordinates $(f(\sigma_b, t), \infty)$.

3.2. Generalizing to higher-dimensional \mathcal{T} . In higher dimensions, we are somewhat limited by the availability of computational geometry data structures and algorithms. When $n = 2$, we use the DCEL data structure to represent the partition of \mathcal{T} into polygons, and we can use one of several algorithms for solving the point-location problem. To the best of my knowledge, there is not an analogous data structure (yet) for storing a partition of a space into n -dimensional polyhedrons for arbitrary $n \geq 3$, and there are not algorithms (yet) for solving the point-location problem in higher dimensions.

Otherwise, the algorithm of Section 3.1 (as outlined at the beginning of Section 3) requires almost no modifications for higher-dimensional \mathcal{T} . The partition of \mathcal{T} into polygons is replaced by a partition of \mathcal{T} into n -dimensional polyhedrons, where $n = \dim(\mathcal{T})$. Only the first step (computing the polyhedrons) requires a meaningful modification, which I describe below.

When $n = 2$, the intersection of $I(\sigma, \tau)$ with a triangle $T \in \mathcal{T}$ is the intersection of a line with T , which is a line segment $L_{\sigma, \tau, T}$. These line segments completely determine the polygonal partition of \mathcal{T} because the line segments are the faces of the polygons. In turn, each line segment $L_{\sigma, \tau, T}$ is completely determined by the intersection of $L_{\sigma, \tau, T}$ with the 1-skeleton of \mathcal{T} ; this intersection is a pair $(v_{\sigma, \tau, T}, w_{\sigma, \tau, T})$ of points. We computed the set $\{(v_{\sigma, \tau, T}, w_{\sigma, \tau, T})\}_{\sigma, \tau, T}$ by restricting the fibered filtration function f to a path through the 1-skeleton of \mathcal{T} and applying the Bentley–Ottman planesweep algorithm.

In general, the intersection of $I(\sigma, \tau)$ with an n -simplex $T \in \mathcal{T}$ is the intersection of an $(n - 1)$ -dimensional hyperplane $H_{\sigma, \tau, T}$ with T , which is an $(n - 1)$ -dimensional polyhedron $P_{\sigma, \tau, T}$. The set $\{P_{\sigma, \tau, T}\}_{\sigma, \tau, T}$ completely determines the polyhedral partition of \mathcal{T} that is given by Proposition 2.4 because the polyhedrons $P_{\sigma, \tau, T}$ are the $(n - 1)$ -dimensional faces of the n -dimensional polyhedrons in the partition. In turn, each polyhedron $P_{\sigma, \tau, T}$ is completely determined by its intersection with the 1-skeleton of \mathcal{T} , as follows. The m -dimensional faces of $P_{\sigma, \tau, T}$ are the set $\{H_{\sigma, \tau, T} \cap F \mid F \text{ is an } (m + 1)\text{-dimensional face of } T \text{ and } H_{\sigma, \tau, T} \cap F \neq \emptyset\}$. For every $(m + 1)$ -dimensional face F of T such that $H_{\sigma, \tau, T} \cap F \neq \emptyset$, the intersection $H_{\sigma, \tau, T} \cap F$ is the m -dimensional polyhedron whose $(m - 1)$ -dimensional faces are the set $\{H_{\sigma, \tau, T} \cap g \mid g \text{ is an } m\text{-dimensional face of } F\}$. By induction, the faces of $P_{\sigma, \tau, T}$ are determined by $\{H_{\sigma, \tau, T} \cap e \mid e \text{ is a 1-dimensional face of } T \text{ (i.e., an edge)}\}$, which are the vertices of $P_{\sigma, \tau, T}$. Consequently, we can compute each $P_{\sigma, \tau, T}$ by computing its vertices. As in the case in which $\dim(\mathcal{T}) = 2$, we do this by restricting the fibered filtration function f to a path through the 1-skeleton of \mathcal{T} and applying the Bentley–Ottman planesweep algorithm.

4. CONCLUSIONS AND DISCUSSION

I introduced an algorithm for efficiently computing PD bundles when the fibered filtration function is piecewise-linear. I gave full implementation details for the case in which the base space \mathcal{T} is 2D, and in Section 3.2 I discussed how one may generalize to higher dimensions. I conclude with some questions and proposals for future work:

- What invariants can we use for summarizing and analyzing PD bundles in ways that do not require exploratory data analysis? The current algorithm requires a user to “query” the PD bundle at various points in the base space.
- Can we generalize the implementation of the algorithm to higher-dimensional base spaces \mathcal{T} ? Generalizing to higher-dimensional base spaces will require generalizing certain computational geometry data structures and algorithms. For example, we must generalize the doubly-connected edge list, which we used to represent a partition of the plane into polygons, to a data structure that can represent a partition of a higher-dimensional space into polyhedrons. Such higher-dimensional computational geometry algorithms may be useful for other applications as well.
- Can we generalize the algorithm to nonpiecewise-linear fibered filtration functions? For piecewise-linear fibered filtration functions, we used the fact that the base space \mathcal{T} can be partitioned into polyhedrons such that there is a single PD “template” (a list of (birth, death) simplex pairs) for each polyhedron. The template can then be used to obtain $PD_p(f_t)$ at any point t in the polyhedron. For “generic” fibered filtration functions, I showed in [6] that the base space \mathcal{T} is stratified such that for each $\dim(\mathcal{T})$ -dimensional stratum, there is a single PD template which can be used to obtain $PD_p(f_t)$ at any point t in the stratum.

ACKNOWLEDGEMENTS

I thank Michael Lesnick and Nina Otter for helpful discussions about the algorithm for computing PD bundles.

APPENDIX

A.1. Technical details of the algorithm. In Section 3.1, we made two generic assumptions to simplify the exposition. If assumption (1) does not hold, then for any triangle T in \mathcal{T} and pair (σ, τ) of simplices, it is possible for $I(\sigma, \tau) \cap T$ to equal T or an edge of T . In Figure 7, we illustrate an example where assumption (1) does not hold. We highlight the line segments on which σ and τ swap (see Definition 3.1). If assumption (2) does not hold, then it is possible for there to be a line segment ℓ in triangle T such that $I(\sigma_1, \tau_1) \cap T = \ell = I(\sigma_2, \tau_2) \cap T$ for two distinct pairs $(\sigma_1, \tau_1), (\sigma_2, \tau_2)$.

In Sections A.1.2 and A.1.3, I explain the modifications for the algorithm when we do not make the assumptions of Section 3.1. Only step 1 (Section 3.1.1) and step 2 (Section 3.1.2) need to be modified.

A.1.1. Preliminaries. As in Section 3.1.1, we traverse a path γ through the 1-skeleton of \mathcal{T} . Once again, the restriction of the fibered filtration function f to γ is a 1-parameter filtration function, and we use the Bentley-Ottman algorithm to find points v on γ at which the relative order of a pair of simplices changes.

Definition A.1. *A vertex v for a pair (σ, τ) of simplices is detected along edge e if, while traversing edge $e \subseteq \gamma$ during the Bentley-Ottman algorithm, we detect the point $v \in e$ as a point where the relative order of σ and τ changes.*

A vertex v for the pair (σ, τ) is detected along edge e if and only if σ and τ have different relative orders at the endpoints of e . If v is an endpoint of e , then v is detected if and only if the relative order at v is different from the relative order in the interior of the edge e .

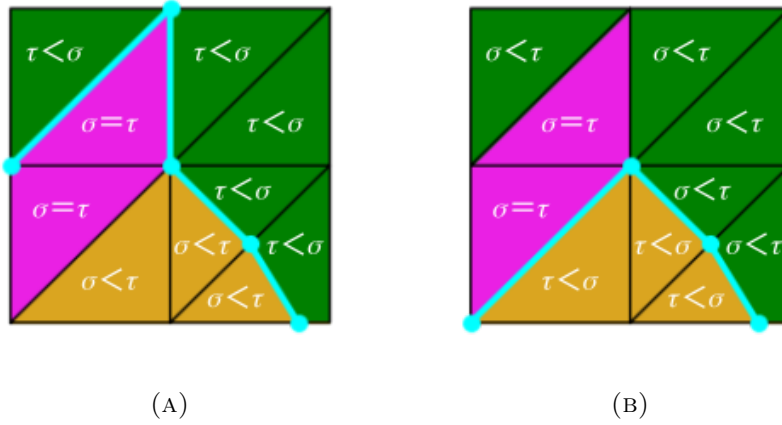


FIGURE 7. Two examples of a fibered filtration function for which assumption (1) of Section 3.1 does not hold. The pair (σ, τ) is a pair of simplices such that $I(\sigma, \tau) \cap T = T$ for every pink triangle T ; the full intersection $I(\sigma, \tau)$ is illustrated in Figure 2d. We assume that $\beta(\sigma) < \beta(\tau)$ in the intrinsic ordering $\beta : \mathcal{K} \rightarrow \{1, \dots, N\}$, which is used to break ties in the simplex ordering whenever two simplices have the same filtration value (see Section 2.3). In blue, we draw the line segments on which the pair (σ, τ) swaps. (A) The case in which $f(\tau) < f(\sigma)$ on green triangles and $f(\sigma) < f(\tau)$ on yellow triangles. (B) The case in which $f(\sigma) < f(\tau)$ on green triangles and $f(\tau) < f(\sigma)$ on yellow triangles.

Definition A.2. A line segment (v, w) is detected in triangle T if there is a pair (σ, τ) of simplices such that vertex v is detected along an edge e_1 of T for (σ, τ) and vertex w is detected along an edge e_2 of T for (σ, τ) .

Lemma A.3, below, characterizes the conditions under which a pair of simplices swaps along a line segment.

Lemma A.3. Let (v, w) be a line segment that is not on the boundary of \mathcal{T} .

- (1) If v and w are not the endpoints of an edge in \mathcal{T} , let T be the unique triangle that contains (v, w) . A pair (σ, τ) of simplices swaps along the line segment (v, w) if and only if (v, w) is detected in triangle T .
- (2) If v and w are the endpoints of an edge in \mathcal{T} , let T_1, T_2 be the two triangles adjacent to that edge. A pair (σ, τ) of simplices swaps along the line segment (v, w) if and only if (v, w) is detected in exactly one of T_1, T_2 .

Proof. Statement (1) is clear. This was the situation in Section 3.1. It remains only to prove statement (2).

Suppose (v, w) are the endpoints of an edge e in \mathcal{T} that is not on the boundary of \mathcal{T} . Let T_1, T_2 be the two triangles adjacent to T . As illustrated in Figure 8a, we denote the third vertex of T_1 by u_1 , the third vertex of T_2 by u_2 , the other two edges in T_1 by e_2, e_3 , and the other two edges in T_2 by e_4, e_5 .

A pair (σ, τ) swaps along (v, w) only if $e \subseteq I(\sigma, \tau) \cap T_1$ and $e \subseteq I(\sigma, \tau) \cap T_2$. If $e \subseteq I(\sigma, \tau) \cap T$ for triangle T , then either $I(\sigma, \tau) \cap T = e$ or $I(\sigma, \tau) \cap T = T$. If we have both $I(\sigma, \tau) \cap T_1 = T_1$

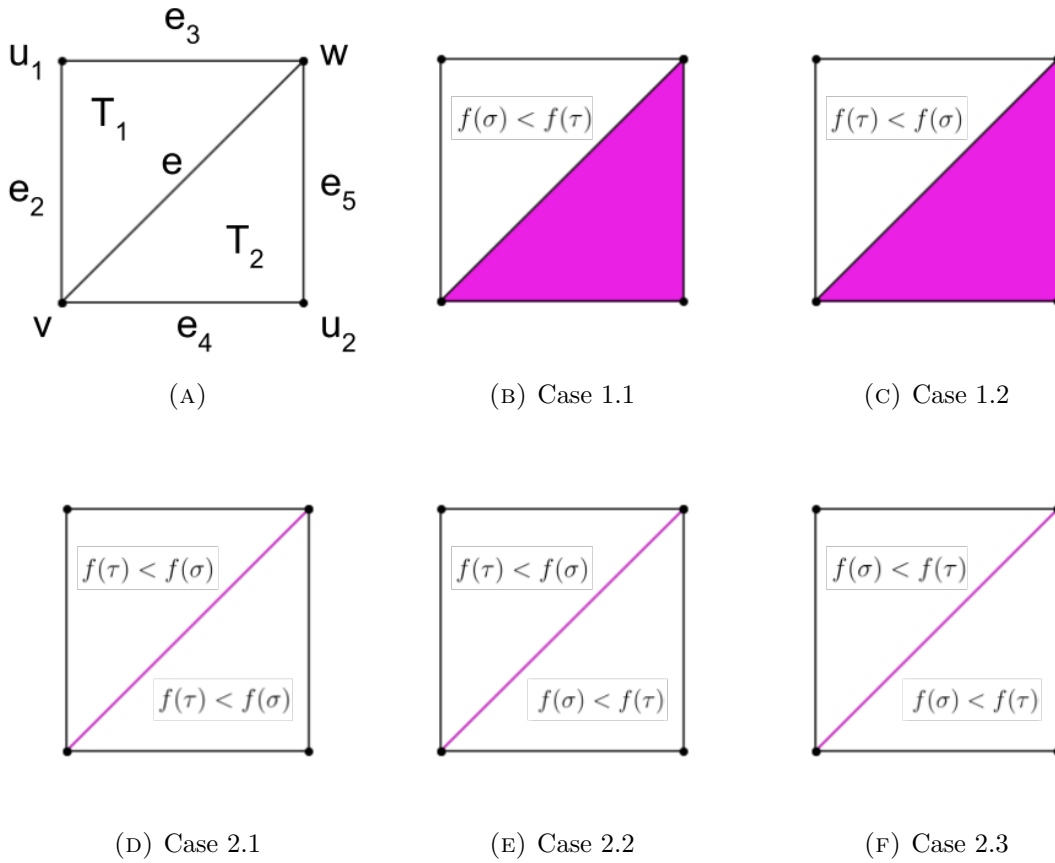


FIGURE 8. (A) The vertices, edges, and triangles defined in the proof of Lemma A.3. (B–F) The casework in the proof of Lemma A.3. The color pink indicates that σ and τ have equal filtration values.

and $I(\sigma, \tau) \cap T_2 = T_2$, then (σ, τ) does not swap along (v, w) because σ and τ have the same relative order in T_1 and T_2 . Therefore, the pair (σ, τ) swaps along (v, w) only if the intersection of $I(\sigma, \tau)$ with one triangle is e and the intersection with the other triangle is either e or the entire triangle. Without loss of generality, $I(\sigma, \tau) \cap T_1 = e$ and either $I(\sigma, \tau) \cap T_2 = T_2$ or $I(\sigma, \tau) \cap T_2 = e$.

The line segment (v, w) can only be detected in triangle T_i if $e = I(\sigma, \tau) \cap T_i$. Without loss of generality, $T_i = T_1$. If $I(\sigma, \tau) \cap T_1 = e$ then we must also have $e \subseteq I(\sigma, \tau) \cap T_2$, so either $I(\sigma, \tau) \cap T_2 = T_2$ or $I(\sigma, \tau) \cap T_2 = e$.

In Figures 8b–8f, we illustrate the possible cases in which $I(\sigma, \tau) \cap T_1 = e$ and either $I(\sigma, \tau) \cap T_2 = T_2$ or $I(\sigma, \tau) \cap T_2 = e$. We will show that in each of these cases, statement (2) holds. In all other cases, we have already shown that neither (σ, τ) swaps along the line segment (v, w) nor is (v, w) detected in T_1 or T_2 .

Recall that when $f(\sigma, t) = f(\tau, t)$, the simplex ordering $\alpha(\cdot, t)$ is not uniquely determined by the filtration function. A fixed “intrinsic ordering” $\beta : \mathcal{K} \rightarrow \{1, \dots, N\}$, discussed in Section 2.3, is used to break ties. Without loss of generality, we assume $\beta(\sigma) < \beta(\tau)$ in the intrinsic ordering. This implies that $\alpha(\sigma, t) < \alpha(\tau, t)$ whenever $t \in I(\sigma, \tau)$.

Case 1: $I(\sigma, \tau) \cap T_2 = T_2$.

There are two subcases.

- (1) **Case 1.1:** (Figure 8b) $f(\sigma, t) \leq f(\tau, t)$ for all $t \in T_1$, with equality only for $t \in e$.

In this subcase, we have $\alpha(\sigma, t) < \alpha(\tau, t)$ for all $t \in T_1 \cup T_2$. Therefore, the pair (σ, τ) does not swap along (v, w) . Neither v nor w is detected along any edges of T_1 or T_2 , so the line segment (v, w) is not detected in either T_1 or T_2 .

- (2) **Case 1.2:** (Figure 8c) $f(\tau, t) \leq f(\sigma, t)$ for all $t \in T_1$, with equality only for $t \in e$.

In this subcase, we have $\alpha(\sigma, t) < \alpha(\tau, t)$ for $t \in T_2$ and $\alpha(\tau, t) < \alpha(\sigma, t)$ for all $t \in T_1 \setminus e$. Therefore, the pair (σ, τ) swaps along (v, w) . The vertex v is detected along edge e_2 and the vertex w is detected along the edge e_3 . Because e_2 and e_3 are edges of T_1 , the line segment (v, w) is detected in T_1 . The vertices v and w are not detected along any edge of T_2 , so (v, w) is not detected in T_2 .

Case 2: $I(\sigma, \tau) \cap T_2 = e$.

There are three subcases.

- (1) **Case 2.1:** (Figure 8d) $f(\tau, t) \leq f(\sigma, t)$ for all $t \in T_1 \cup T_2$, with equality only for $t \in e$.

In this subcase, we have $\alpha(\tau, t) < \alpha(\sigma, t)$ for all $t \in (T_1 \cup T_2) \setminus e$. Therefore, the pair (σ, τ) does not swap along (v, w) . The vertex w is detected along edges e_3 and e_5 . The vertex v is detected along edges e_2 and e_4 . Therefore, (v, w) is detected in both T_1 and T_2 .

- (2) **Case 2.2:** (Figure 8e) Either $f(\tau, t) \leq f(\sigma, t)$ for all $t \in T_1$ and $f(\sigma, t) \leq f(\tau, t)$ for all $t \in T_2$, or $f(\sigma, t) \leq f(\tau, t)$ for all $t \in T_1$ and $f(\tau, t) \leq f(\sigma, t)$ for all $t \in T_1$. Without loss of generality, we assume the former.

In this subcase, $\alpha(\sigma, t) < \alpha(\tau, t)$ for all $t \in T_2$ and $\alpha(\tau, t) < \alpha(\sigma, t)$ for all $t \in T_1 \setminus e$. Therefore, the pair (σ, τ) swaps along (v, w) . The vertex v is detected along e_2 and the vertex w is detected along e_3 , so (v, w) is detected in triangle T_1 . Neither v nor w is detected along any edge of T_2 , so (v, w) is not detected in T_2 .

- (3) **Case 2.3:** (Figure 8f) $f(\sigma, t) \leq f(\tau, t)$ for all $t \in T_1 \cup T_2$, with equality only for $t \in e$.

In this subcase, we have $\alpha(\sigma, t) < \alpha(\tau, t)$ for all $t \in T_1 \cup T_2$. Therefore, the pair (σ, τ) does not swap along (v, w) . Neither v nor w is detected along any edge of T_1 or T_2 , so (v, w) is not detected in either T_1 or T_2 .

□

Lemma A.4 below will be used to modify step 2 of the algorithm: computing the simplex pairing function.

Lemma A.4. *Let $\alpha_0, \alpha_1 : \mathcal{K} \rightarrow \{1, \dots, N\}$ denote two different simplex orderings, where N is the number of simplices in \mathcal{K} . Let $\{(\sigma_i, \tau_i)\}_{i=1}^m$ be the set of pairs (σ_i, τ_i) such that $(\alpha_0(\sigma_i) - \alpha_0(\tau_i))(\alpha_1(\sigma_i) - \alpha_1(\tau_i)) < 0$, i.e., σ_i and τ_i have different relative orders in α_0 and α_1 . Let $\zeta_0 := \alpha_0$, and for $i = 1, \dots, m$, let $\zeta_i : \mathcal{K} \rightarrow \{1, \dots, N\}$ be the simplex ordering obtained by transposing (σ_i, τ_i) in the simplex ordering ζ_{i-1} . If $\zeta_{i-1}(\sigma_i)$ and $\zeta_{i-1}(\tau_i)$ are*

consecutive integers for all i , then $\zeta_m = \alpha_1$. Furthermore, the sequence $\{(\sigma_i, \tau_i)\}_{i=1}^m$ can be ordered so that this conditions holds.

Proof. First, we prove that there is at least one pair (σ_i, τ_i) such that $\alpha_0(\sigma_i)$ and $\alpha_0(\tau_i)$ are consecutive integers. Let $i = \arg \min_j \|\alpha_0(\sigma_j) - \alpha_0(\tau_j)\|$. For a contradiction, suppose that $j_1 := \alpha_0(\sigma_i)$ and $j_2 := \alpha_0(\tau_i)$ are not consecutive integers. Without loss of generality, $j_1 < j_2$. For $r = 1, \dots, j_2 - j_1 - 1$, let $\rho_{j_1+r} := \alpha_0^{-1}(j_1 + r)$ (i.e., $\rho_{j_1+1}, \dots, \rho_{j_2-1}$ are the simplices between σ_i and τ_i). For all r , we must have that either $(\sigma_i, \rho_{j_1+r}) \in \{(\sigma_k, \tau_k)\}_{k=1}^m$ or $(\tau_i, \rho_{j_1+r}) \in \{(\sigma_k, \tau_k)\}_{k=1}^m$ (i.e., either the relative order of σ_i and ρ_{j_1+r} changes or the relative order of τ_i and ρ_{j_1+r} changes). By definition of i , we must have that none of $(\rho_{j_1+r_1}, \rho_{j_1+r_2})$ are in $\{(\sigma_k, \tau_k)\}_{k=1}^m$ (i.e., the relative order of the simplices $\rho_{j_1+1}, \dots, \rho_{j_2-1}$ doesn't change). Therefore we must either have $(\sigma_i, \rho_{j_1+1}) \in \{(\sigma_k, \tau_k)\}_{k=1}^m$ or $(\tau_i, \rho_{j_1+r}) \in \{(\sigma_k, \tau_k)\}_{k=1}^m$ for all r . In either case, one of these is a transposition of simplices whose indices in the ordering are consecutive integers, which is a contradiction.

Now we prove the lemma by induction on m . When $m = 1$, we showed above that $\alpha_0(\sigma_1)$ and $\alpha_0(\tau_1)$ are consecutive integers. Clearly $\zeta_1 = \alpha_1$. In the general case, we can assume $\alpha_0(\sigma_1)$ and $\alpha_0(\tau_1)$ are consecutive integers without loss of generality. The set $\{(\sigma_i, \tau_i)\}_{i=2}^m$ is the set of pairs (σ_i, τ_i) such that $(\zeta_1(\sigma_i) - \zeta_1(\tau_i))(\alpha_1(\sigma_i) - \alpha_1(\tau_i)) < 0$, i.e., σ_i and τ_i have different relative orders in ζ_1 and α_1 for all $i = 2, \dots, m$. By induction, we can assume $\{(\sigma_i, \tau_i)\}_{i=2}^m$ is ordered such that $\zeta_{i-1}(\sigma_i)$ and $\zeta_{i-1}(\tau_i)$ are consecutive integers for $i = 2, \dots, m$ and $\zeta_m = \alpha_1$. \square

A.1.2. Modifications to step 1: Computing the polygons. In Section 3.1.1, we maintained a dictionary $\mathcal{D}_1(T)$ for each triangle $T \in \mathcal{T}$. The keys were pairs (σ, τ) such that $I(\sigma, \tau) \cap T$ was a line segment in T , and the value of (σ, τ) was the list $[v, w]$ of vertices in $\mathcal{A}(L)$ that were the endpoints of the line segment $I(\sigma, \tau) \cap T$.

Now we maintain two additional dictionaries $\mathcal{D}_2(T)$ and $\mathcal{D}_3(T)$ for each triangle $T \in \mathcal{T}$. These dictionaries are initialized to be empty, and are updated as we traverse the path γ through the 1-skeleton of \mathcal{T} . At any point in the traversal of γ , the keys of $\mathcal{D}_2(T)$ are pairs (v, w) of vertices in $\mathcal{A}(L)$ such that

- (1) The line segment (v, w) has been detected in T .
- (2) The line segment (v, w) is not an edge of T .

The value of $\mathcal{D}_2(T)[(v, w)]$ is a list $[(\sigma_1, \tau_1), \dots, (\sigma_m, \tau_m)]$ of the simplex pairs that we have found so far such that σ_i and τ_i swap along (v, w) . The keys of $\mathcal{D}_3(T)$ are vertices $v \in \mathcal{A}(L)$ such that

- (1) Vertex v has been detected along an edge e of triangle T .
- (2) There is a pair (σ, τ) of simplices such that (σ, τ) swaps at v and we have not yet found a vertex w such that $I(\sigma, \tau) \cap T = (v, w)$.

The algorithm of Section 3.1.1 is modified as follows. Suppose we are traversing the path γ through the 1-skeleton of \mathcal{T} and we detect a vertex v along edge e for the set $\{(\sigma_1, \tau_1), \dots, (\sigma_m, \tau_m)\}$ of simplex pairs. We do the following:

- (1) **Update \mathcal{D}_1 :** For each triangle $T \in \mathcal{T}$ that is adjacent to e , we append v to the list of vertices for $\mathcal{D}_1(T)[(\sigma_i, \tau_i)]$ for all i , as in Section 3.1.1.
- (2) **Update $\mathcal{A}(L)$:** If v is not an endpoint of e , we split the edge e in $\mathcal{A}(L)$ and add a vertex within e , as in Section 3.1.1. If v is an endpoint of e , we do not split the edge or create a new vertex because \mathcal{T} already has a vertex at v .

- (3) **Update \mathcal{D}_2 , \mathcal{D}_3 , and edge labels:** For each triangle T adjacent to e and each (σ_i, τ_i) :
- If v is the only vertex in the list $\mathcal{D}_1(T)[(\sigma_i, \tau_i)]$, then we have not yet detected a line segment for (σ_i, τ_i) of the form (v, w) , for any vertex w . We do the following: If v is not in $\mathcal{D}_3(T)$, add key v to $\mathcal{D}_3(T)$ with value $[(\sigma_i, \tau_i)]$. Otherwise, append (σ_i, τ_i) to $\mathcal{D}_3(T)[v]$.
 - Otherwise, there is another vertex $w \in \mathcal{D}_1(T)[(\sigma_i, \tau_i)]$. This means we have just detected a line segment (v, w) in T for (σ_i, τ_i) . We remove (σ_i, τ_i) from $\mathcal{D}_3(T)[w]$.
 - If v and w are not both vertices of \mathcal{T} , then (v, w) is not an edge of \mathcal{T} . We do the following: If (v, w) is not in $\mathcal{D}_2(T)$, then add key (v, w) to $\mathcal{D}_2(T)$ with value $[(\sigma_i, \tau_i)]$. Otherwise, append (σ_i, τ_i) to $\mathcal{D}_2(T)[(v, w)]$.
 - Otherwise, v and w are both vertices of triangle T . This means we have detected a line segment (v, w) in T in which v and w are the endpoints of an edge e' in \mathcal{T} . If e' is an edge on the boundary of \mathcal{T} , then we do nothing. Otherwise, let T_2 be the other triangle adjacent to e' . By Lemma A.3, the pair (σ_i, τ_i) swaps along (v, w) if and only if the line segment is not detected in T_2 . If e' already stores a reference to (σ_i, τ_i) , then we remove it because this implies that e' was detected in T_2 already. Otherwise, we add a reference to (σ_i, τ_i) on e' .

When the traversal of the 1-skeleton is done, we add lines to $\mathcal{A}(L)$. For every triangle $T \in \mathcal{T}$ and every key $(v, w) \in \mathcal{D}_2(T)$, we add a line segment with endpoints v, w to the DCEL that represents $\mathcal{A}(L)$. For every edge in the DCEL that is a subset of the line segment (v, w) , we label the edge with a reference to the list $\mathcal{D}_2(T)[(v, w)]$, which is the list $\{(\sigma_1, \tau_1), \dots, (\sigma_m, \tau_m)\}$ of simplex pairs that swap along the line segment.

A.1.3. Modifications to step 2: Computing the pairing function. We compute a path Γ as in Section 3.1.2 and traverse Γ . At each step, we walk from one polygon P_1 to the next polygon P_2 by crossing an edge e in $\mathcal{A}(L)$. The edge e stores a list of simplex pairs (σ, τ) such that σ and τ have different relative orders in the polygons P_1, P_2 . We update the simplex ordering one transposition at a time. Let $\bar{\alpha} : \mathcal{K} \rightarrow \{1, \dots, N\}$ denote the current ordering, which we initialize to the simplex ordering $\alpha(\cdot, P_1)$ in P_1 . While the list that e stores is nonempty, we do the following:

- (1) Let (σ, τ) be the first element of the list.
- (2) If $\bar{\alpha}(\sigma)$ and $\bar{\alpha}(\tau)$ are consecutive integers, then we update $\bar{\alpha}$ by swapping the order of σ and τ . As in Section 3.1.2, we update the simplex ordering, the RU decomposition, and the (birth, death) simplex pairs. We remove (σ, τ) from the list.
- (3) Otherwise, we move (σ, τ) to the end of the list.

At the end of this algorithm, $\bar{\alpha}$ is the simplex ordering $\alpha(\cdot, P_2)$ in P_2 (by Lemma A.4), the RU decomposition is an RU decomposition for P_2 , and we have computed the (birth, death) simplex pairs for P_2 .

A.2. Triangulation of a hyper-rectangle. In Section 2.3, we discussed that one can construct a piecewise-linear fibered filtration function by linear interpolation of a set $\{f_v : \mathcal{K} \rightarrow \mathbb{R}\}_{v \in \prod_{i=1}^m \mathcal{I}_i}$ of filtration functions, where \mathcal{I}_i is a finite set of real numbers for $i = 1, \dots, m$. To do this, we must construct a triangulation of $\prod_{i=1}^m [\min \mathcal{I}_i, \max \mathcal{I}_i]$ whose vertices are the elements of $\prod_{i=1}^m \mathcal{I}_i$. Let $\{a_i^j\}_j$ be the sequence of elements in \mathcal{I}_i , such that $a_i^j < a_i^{j+1}$

for all j . To triangulate $\prod_{i=1}^m \mathcal{I}_i$, it suffices to triangulate each $\prod_{i=1}^m [a_i^{j_i}, a_i^{j_i+1}]$ for all sequences j_1, \dots, j_m . We do this inductively on m . When $m = 1$, the interval $[a_i^{j_i}, a_i^{j_i+1}]$ is a 1-simplex and thus already triangulated. Suppose that $\prod_{i=1}^{m-1} [a_i^{j_i}, a_i^{j_i+1}]$ is triangulated; that is, we have $\prod_{i=1}^{m-1} [a_i^{j_i}, a_i^{j_i+1}] = \bigcup_k \Delta_k^{m-1}$, where Δ_k^{m-1} is an $(m-1)$ -simplex for all k . Thus $\prod_{i=1}^m [a_i^{j_i}, a_i^{j_i+1}] = \bigcup_k \left(\Delta_k^{m-1} \times [a_m^{j_m}, a_m^{j_m+1}] \right)$. For all k , the product $\Delta_k^{m-1} \times [a_m^{j_m}, a_m^{j_m+1}]$ can be triangulated as in the proof of Theorem 2.10 in [5]. This yields

$$\prod_{i=1}^m [a_i^{j_i}, a_i^{j_i+1}] = \bigcup_k \left(\Delta_k^{m-1} \times [a_m^{j_m}, a_m^{j_m+1}] \right) = \bigcup_k \bigcup_\ell \Delta_{k\ell}^m,$$

where $\bigcup_\ell \Delta_{k\ell}^m$ is the triangulation of $\Delta_k^{m-1} \times [a_m^{j_m}, a_m^{j_m+1}]$.

REFERENCES

- [1] David Cohen-Steiner, Herbert Edelsbrunner, and Dmitriy Morozov. Vines and vineyards by updating persistence in linear time. In *Proceedings of the Twenty-Second Annual Symposium on Computational Geometry*, SCG '06, pages 119–126, New York, NY, USA, 2006. Association for Computing Machinery.
- [2] Mark de Berg, Otfried Cheong, Marc van Kreveld, and Mark Overmars. *Computational Geometry: Algorithms and Applications*. Springer, Berlin, Heidelberg, 3rd edition, 2008.
- [3] Herbert Edelsbrunner and John Harer. *Computational Topology: An Introduction*. American Mathematical Society, Providence, RI, 2010.
- [4] Herbert Edelsbrunner, David Letscher, and Afra Zomorodian. Topological persistence and simplification. *Discrete & Computational Geometry*, 28:511–533, 2002.
- [5] Allen Hatcher. *Algebraic Topology*. Cambridge University Press, Cambridge, UK, 1st edition, 2001.
- [6] Abigail Hickok. Persistence diagram bundles: A multidimensional generalization of vineyards. *arXiv:2210.05124*, 2022.
- [7] Michael Lesnick and Matthew Wright. Interactive visualization of 2-D persistence modules. *arXiv:1512.00180*, 2015.
- [8] Yanjie Li, Dingkan Wang, Giorgio A. Ascoli, Partha Mitra, and Yusu Wang. Metrics for comparing neuronal tree shapes based on persistent homology. *PLoS ONE*, 12(8):e0182184, 2017.
- [9] Nina Otter, Mason A. Porter, Ulrike Tillmann, Peter Grindrod, and Heather A. Harrington. A roadmap for the computation of persistent homology. *EPJ Data Science*, 6:17, 2017.
- [10] Neil Sarnak and Robert E. Tarjan. Planar point location using persistent search trees. *Communications of the ACM*, 29(7):669–679, 1986.
- [11] Robert Sedgewick and Kevin Wayne. *Algorithms*, chapter 4.3, pages 604–637. Addison–Wesley, 4th edition, 2011.
- [12] Csaba D. Toth, Joseph O’Rourke, and Jacob E. Goodman. *Handbook of discrete and computational geometry*. CRC Press, Boca Raton, FL, 3rd edition, 2017.
- [13] Katharine Turner, Sayan Mukherjee, and Doug M. Boyer. Persistent homology transform for modeling shapes and surfaces. *Information and Inference: A Journal of the IMA*, 3(4):310–344, 2014.